Molecular Biology of the Cell
Vol. 21, 2894–2904, August 15, 2010

Quantitative Analysis of the Mechanism of Endocytic Actin Patch Assembly and Disassembly in Fission Yeast

Vladimir Sirotkin,*† Julien Berro,*‡§ Keely Macmillan,* Lindsey Zhao,* and Thomas D. Pollard*‖¶

Departments of *Molecular, Cellular and Developmental Biology; ‖Molecular Biophysics and Biochemistry; and ¶Cell Biology, Yale University, New Haven, CT 06520-8103; and ‡Institut Camille Jordan, UMR CNRS 5208, and §Centre de Génétique Moléculaire et Cellulaire, UMR CNRS 5534, Université Lyon 1, F-69622 Villeurbanne Cedex, France

Submitted February 24, 2010; Accepted June 17, 2010
Monitoring Editor: Sandra L. Schmid

We used quantitative confocal microscopy to measure the numbers of 16 proteins tagged with fluorescent proteins during assembly and disassembly of endocytic actin patches in fission yeast. The peak numbers of each molecule that accumulate in patches varied <30–50% between individual patches. The pathway begins with accumulation of 30–40 clathrin molecules, sufficient to build a hemisphere at the tip of a plasma membrane invagination. Thereafter precisely timed waves of proteins reach characteristic peak numbers: endocytic adaptor proteins (~120 End4p and ~230 Pan1p), activators of Arp2/3 complex (~200 Wsp1p and ~340 Myo1p) and ~300 Arp2/3 complexes just ahead of a burst of actin assembly into short, capped and highly cross-linked filaments (~7000 actins, ~200 capping proteins, and ~900 fimbrins). Coronin arrives last as all other components disperse upon patch internalization and movement over ~10 s. Patch internalization occurs without recruitment of dynamins. Mathematical modeling, described in the accompanying paper (Berro *et al.*, 2010, MBoC *21*: 2803–2813), shows that the dendritic nucleation hypothesis can account for the time course of actin assembly into a branched network of several hundred filaments 100–200 nm long and that patch disassembly requires actin filament fragmentation in addition to depolymerization from the ends.

INTRODUCTION

Clathrin-dependent endocytosis in yeast cells depends on the assembly of structures called actin patches (Kaksonen *et al.*, 2006; Galletta and Cooper, 2009), which are associated with tubular invaginations of the plasma membrane 50 nm in diameter and up to 180 nm long in budding yeast (Mulholland *et al.*, 1994; Idrissi *et al.*, 2008). The protein composition of actin patches evolves along a precisely timed pathway (Kaksonen *et al.*, 2003, 2005; Sirotkin *et al.*, 2005), beginning with recruitment of clathrin and endocytic adaptor proteins at the tip of a shallow invagination of the plasma membrane, followed by recruitment of activators of Arp2/3 complex to the base and side of the invagination (Kaksonen *et al.*, 2003, 2005; Newpher *et al.*, 2005; Idrissi *et al.*, 2008). Arp2/3 complex stimulates rapid assembly of branched actin filaments (Young *et al.*, 2004) and associated proteins into a network surrounding a deepening invagination of the plasma membrane (Rodal *et al.*, 2005; Idrissi *et al.*, 2008). Actin assembly may provide force for membrane invagination, endocytic vesicle scission, or vesicle propulsion, although questions remain about each of these possible functions (Merrifield, 2004; Galletta and Cooper, 2009). As in animal cells (Merrifield *et al.*, 2005) the patch moves away from the plasma membrane when the endocytic vesicle is severed from the plasma membrane and internalized (Huckaba *et al.*, 2004; Toshima *et al.*, 2006). As they move, patches lose actin filaments and other proteins.

Although the order of protein assembly in endocytic actin patches is established for budding yeast (Kaksonen *et al.*, 2003, 2005) and the average number of molecules for eight proteins in actin patches is known in fission yeast (Wu and Pollard, 2005), many critical aspects of the mechanism are still unclear, including regulation of vesicle coat assembly, mechanism of actin filament assembly and disassembly and the detailed organization of the proteins around the invaginating membrane (Kaksonen *et al.*, 2006; Galletta and Cooper, 2009). Electron microscopy (Young *et al.*, 2004; Rodal *et al.*, 2005) showed that patches contain short, branched filaments, consistent with dendritic nucleation by Arp2/3 complex (Pollard *et al.*, 2000). However, the available evidence falls far short of verifying that this mechanism actually accounts for actin assembly in a live cell.

As in any complex biochemical pathway, understanding underlying mechanisms requires knowledge of cytoplasmic concentrations of the participating proteins, rate constants for the reactions, and quantitative measurements of the behavior of the molecules over time in live cells. To obtain data to test quantitative models of actin patch assembly, we measured the time courses of the accumulation and loss of 16 proteins associated with endocytic actin patches in fission yeast. We tagged these patch components with fluorescent proteins and used a calibrated confocal microscope (Wu and Pollard, 2005) to measure for each protein the cytoplasmic

This article was published online ahead of print in *MBoC in Press* (http://www.molbiolcell.org/cgi/doi/10.1091/mbc.E10–02–0157) on June 29, 2010.

† Present address: Department of Cell and Developmental Biology, SUNY Upstate Medical University, 750 E. Adams Street, Syracuse, NY 13210.

Address correspondence to: Thomas D. Pollard (thomas.pollard@yale.edu).

concentration and the numbers of molecules in patches. The stoichiometry of actin patch components provides direct insights into actin patch architecture. The kinetics of the appearance and disappearance of these proteins provide the information required to constrain mathematical models of the process.

In the accompanying article (Berro *et al.*, 2010) we use mathematical modeling to show that the mechanism described by the dendritic nucleation hypothesis (Pollard *et al.*, 2000) can account for the actin patch assembly and disassembly and to determine the reaction parameters required to fit the live cell measurements. We find that patch assembly requires higher rates of filament capping and actin filament branching than observed in dilute solution and that disassembly of the network requires actin filament severing by cofilin and loss of actin filament fragments by diffusion in addition to depolymerization.

MATERIALS AND METHODS

Yeast Strains

Table S1 lists all *Schizosaccharomyces pombe* strains used in this study. Fluorescent protein (FP) tag sequences were integrated into the genome by PCR-based gene tagging (Bahler *et al.*, 1998) in haploid strains for all markers except actin, which was tagged in diploid strains. All proteins except capping protein (Acp2p), twinfilin (Twf1p), and verprolin (Vrp1p) were tagged with monomeric (m) fluorescent proteins (Zacharias *et al.*, 2002). Myosin-1 (Myo1p), Wiskott-Aldrich syndrome protein (WASp, Wsp1p), and actin (Act1p) were tagged on their N-termini. All other proteins were tagged at their C-termini. For C-terminal tagging, the stop codon of a targeted gene was replaced with a pFA6a-GFP(S65T)-kanMX6 cassette or its monomeric fluorescent protein derivative. For N-terminal tagging of Myo1p and Wsp1p, a 100–200-nt 5′ UTR region of the targeted gene was replaced with a monomeric fluorescent protein derivative of pFA6-kanMX6-P3nmt1-green fluorescent protein (GFP) cassette in which *nmt1* promoter was replaced with the native promoter of the targeted gene (Sirotkin *et al.*, 2005). For N-terminal tagging of actin, a 173-nt 5′ UTR region of one of the act1$^+$ genes in a diploid strain was replaced with a monomeric fluorescent protein derivative of pFA6-kanMX6-P3nmt1-GFP cassette. Fim1p was tagged at the C-terminus with mCherry using the pKS391-tagging cassette (Snaith *et al.*, 2005). PCR and microscopy of strains with integrated fluorescent protein sequences confirmed correct integrations. Strains combining two fluorescent protein tags or a fluorescent protein tag and the *myo1* deletion were generated by genetic crosses and tetrad analysis. To facilitate crosses, Δ*myo1* strains contained pUR19 plasmid with wild-type *myo1*$^+$, which was lost upon sporulation.

Microscopy

Cells were grown in YE5S at 25°C to OD595 = 0.2–0.5, washed in EMM, and mounted on pads of 25% gelatin in EMM (Wu *et al.*, 2008). Fluorescence images were acquired using ORCA-ER CCD (Hamamatsu, Bridgewater, NJ) on an UltraView RS (Perkin Elmer, Waltham, MA) spinning disk confocal system installed on Olympus IX-71 microscope with a 100×, 1.4 NA Plan Apo lens (Melville, NY). Z-series at a single time point or time series in a single confocal section were collected for yellow fluorescent protein (YFP) concentration measurements. Time series of Z-stacks were collected for GFP measurements. Z-series through the entire cell depth were acquired in 0.6-μm steps. Images in time series were acquired every 2–3 s for 40–60 s or, for

Table 1. Concentrations and timing of assembly of actin patch components

Common name	Protein name	Concentration in cytoplasm (μM)[a]	Fraction in cytoplasm (%)[a]	Mean peak no. of molecules per patch[b]	No. of seconds to			Lifetime (s)[b]	Total distance (μm)[b]
					Peak (s)[b]	Appearance (s)[b]	Disappearance (s)[b]		
Clathrin heavy chain	Chc1p	0.8	26	40 (±10)		−100 (±27)	<+10	110 (±29)	0.3 (±0.1)
Clathrin light chain	Clc1p	0.7	29	40 (±10)		−105 (±10)	<+10	115 (±10)	0.1 (±0.1)
Sla2 (~Hip1R)	End4p	1.0	72	160 (±20)	−2 (±4)	−32 (±7)	+9 (±3)	41 (±8)	0.7 (±0.3)
Pan1 (~Eps15)	Pan1p	1.0	59	260 (±60)	0 (±3)	−32 (±8)	+9 (±4)	41 (±8)	0.6 (±0.3)
WASp[c]	Wsp1p	4.0	94	230 (±70)	−2 (±1)	−10 (±2)	+2 (±1)	12 (±2)	0.2 (±0.1)
Verprolin	Vrp1p	1.0	87	140 (±10)	−3 (±3)	−9 (±5)	+2 (±2)	11 (±2)	0.2 (±0.1)
Myosin-1	Myo1p	3.3	84	400 (±90)	−2[d]	−9 (±2)[d]	+5 (±2)[d]	14 (±2)	0[d]
Arp2/3 complex[c]	Arp2	2.3	78	320 (±100)	0 (±2)	−13 (±2)	+13 (±3)	26 (±2)	1.3 (±0.2)
	Arp3	3.6	86	320 (±50)	−1 (±3)	−15 (±2)	+11 (±1)	26 (±2)	0.8 (±0.2)
	ARPC5	1.3	67	320 (±60)	−3 (±2)	−15 (±2)	+11 (±2)	26 (±3)	1.2 (±0.3)
Fimbrin	Fim1p	3.7	68	910 (±170)	−1 (±1)	−7 (±1)	+15 (±3)	22 (±2)	1.0 (±0.2)
Capping protein	Acp2p	0.8	66	230 (±60)	0 (±3)	−9 (±2)	+11 (±2)	20 (±3)	0.7 (±0.3)
App1p	App1p	1.2	76	150 (±50)	0 (±2)	−7 (±1)	+8 (±2)	15 (±2)	0.7 (±0.2)
Coronin	Crn1p	3.1	73	490 (±180)	+5 (±3)	−6 (±2)	+15 (±3)	21 (±3)	1.3 (±0.5)
Twinfilin	Twf1p	1.4	65	210 (±40)	+1 (±2)	−7 (±2)	+10 (±4)	17 (±4)	0.8 (±0.3)
Actin,[c,e] 6%	Actin[h]	1.3	65	450 (±90)	+1 (±2)	−9 (±2)	+10 (±2)	19 (±2)	0.7 (±0.2)

See Tables S2 and S3 for more details.

[a] For most proteins the fraction in the cytoplasm was calculated from Z-series of YFP images of entire cells at a single time point. For twinfilin and actin the cytoplasmic fractions were calculated from Z-series of GFP images. For clathrin heavy and light chains, twinfilin and actin, the cytoplasmic fractions were calculated from the ratio of average mean cytoplasmic fluorescence to mean whole cell fluorescence. For all other proteins, the cytoplasmic fraction for a cell was 1 minus the ratio of total fluorescence in patches to total cell fluorescence (see Table S3).

[b] For most proteins, we measured the peak number of molecules per patch, time of peak, appearance and disappearance, total lifetime and distance moved using GFP in time series of Z-stacks spanning entire cells and using YFP in time series in single confocal sections (see Table S2 for comparison). The values in this Table are from GFP measurements in Z-stacks for all proteins except clathrin, for which the values are from YFP measurements in single sections. Measurements of times of appearance, disappearance, and total distance moved were restricted to moving patches.

[c] These fluorescent proteins are not fully functional; the text explains their minor defects.

[d] For Myo1p, time of appearance and disappearance were calculated after aligning Myo1p peak to Wsp1p peak.

[e] Expressed at the level representing 6% of total actin.

clathrin, every 10–20 s for 180–360 s. The exposure times were 50 ms for GFP- and 200 ms for YFP-tagged proteins, except for clathrin, which was imaged with 400-5000-ms exposures. For two-color imaging, cyan fluorescent protein (CFP) and YFP images in time or Z-series were acquired sequentially. Data in TIFF format were transferred to ImageJ (http://rsb.info.nih.gov/ij/) for analysis. In two-color imaging, normalized patch intensity and distances were determined and plotted as described (Sirotkin *et al.*, 2005). The two-color images of dynamin-like proteins and fimbrin in Figure 3 were acquired with an UltraView VoX (Perkin Elmer) spinning disk confocal system equipped with C9100–50 EMCCD camera (Hamamatsu) on a Nikon Ti-E microscope (Melville, NY) with a 100×, 1.4 NA Plan Apo lens (Nikon/MVI).

Data Analysis

We constructed calibration curves using seven proteins (Fim1p, Arp3, Arp2, ARPC5, Acp2p, Myo2p, and Ain1p) whose concentrations were measured by immunoblotting (Wu and Pollard, 2005; Wu *et al.*, 2008). Mean fluorescence intensities per whole cell area in a single section (YFP) or entire Z-series (YFP and GFP) were measured for 3–10 cells, averaged, subtracted for background (mean fluorescence intensity of wild-type cells), and plotted versus number of molecules in an average 92-μm^3 haploid cell. Calibration curves using 2D data were adjusted based on the 3D measurements that determined that a single confocal section through the middle of a cell contained 11% of total cell fluorescence. Calibration curves were used to convert mean fluorescence intensities of unknown proteins into total numbers of molecules per cell or into numbers of molecules in patches.

Local concentrations of proteins in patches were determined by tracking mean fluorescence intensity and position using a six-pixel wide ImageJ circular selection tool centered on each patch. In 3D, each patch was measured in three consecutive confocal sections, and the middle of the three sections contained 51% of total patch fluorescence for all markers examined. Mean cytoplasmic intensities for each cell were measured using a six-pixel wide circular selection tool in several areas away from the patches and subtracted

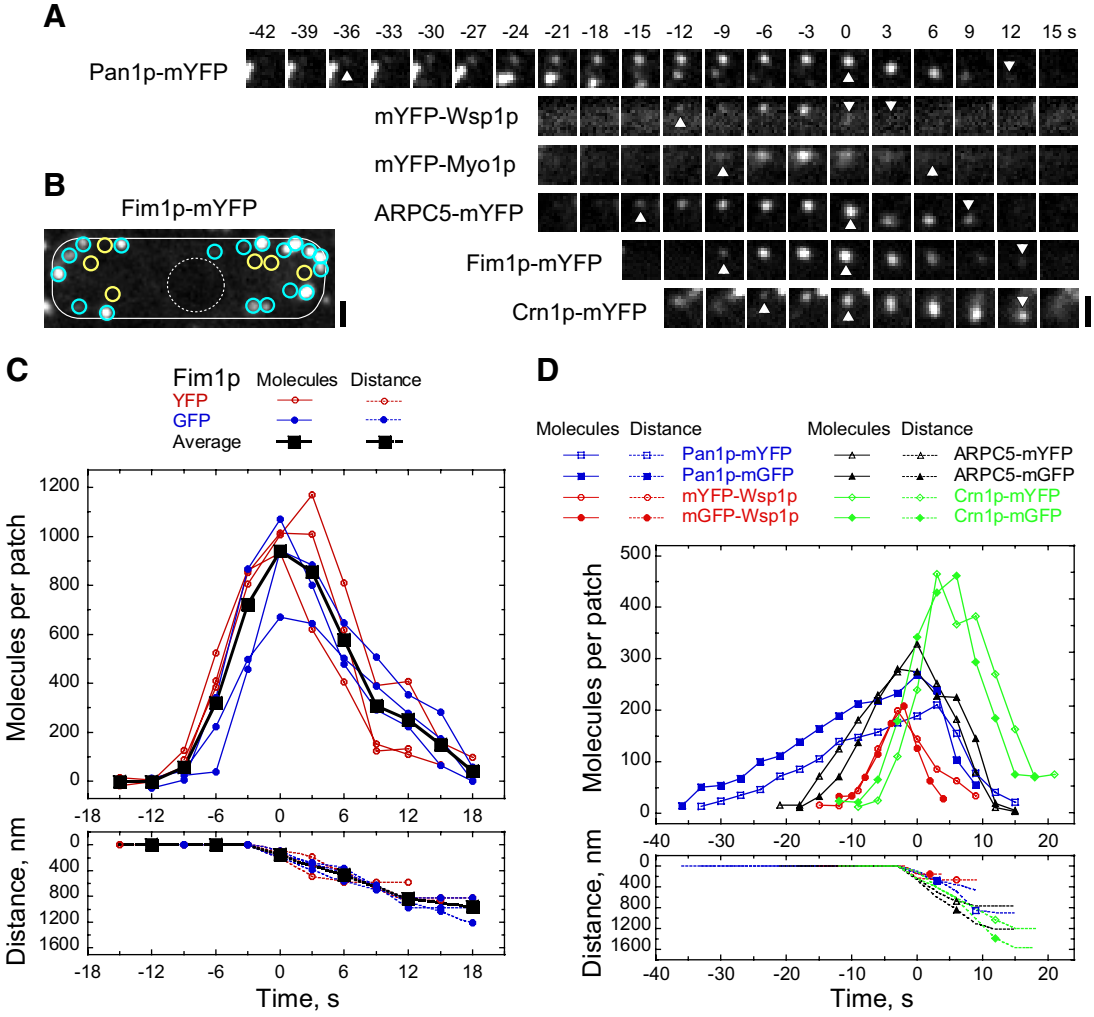

Figure 1. Time courses of protein accumulation and loss in endocytic patches. (A) Time series of micrographs showing the accumulation and loss of YFP-labeled Pan1p, Wsp1p, Myo1p, ARPC5, Fim1p, and Crn1p in individual patches. Confocal fluorescence images through the middle of cells were collected every 3 s. Arrowheads mark the appearance, movement (except for Myo1p) and disappearance of each component. (B) A micrograph of a single confocal section through the middle of a cell expressing Fim1p-mYFP showing areas selected as patches (blue circles) and cytoplasmic background (yellow circles). Solid white line shows cell outline, and dashed white line outlines the nucleus. Scale bars, 1 μm. (C) Comparison and averaging of raw time courses for the number of molecules of YFP-labeled (red, ○) and GFP-labeled (blue, ●) fimbrin Fim1p in individual patches. Averaged time courses (black, ■) were produced by aligning individual time courses to time 0, when patch initiated movement, and averaging at each time point the molecules per patch (top panel, solid lines) and distances traveled by patches (bottom panel, dashed lines). (D) Comparison of average time courses obtained with YFP-labeled proteins (open symbols) and GFP-labeled proteins (closed symbols). Solid lines in the top panel are the average number of molecules per patch, and dashed lines in the bottom panel are distances traveled for Pan1p (blue squares), Wsp1p (red circles), ARPC5 (black triangles), and Crn1p (green diamonds) associated with patches. Each time course is an average of data from three to seven patches. In C and D the numbers of GFP-labeled proteins were calculated from time-lapse movies of Z-sections through entire cells, and the numbers of YFP-labeled proteins were calculated from time-lapse movies in single sections through the middle of cells.

from the mean fluorescence intensities in the six-pixel wide areas of each patch. Distribution of each protein between patches and cytoplasm was calculated by either taking the ratio of total cytoplasm-subtracted fluorescence of all patches in a cell to total cell fluorescence or by calculating the ratio of mean cytoplasmic fluorescence to the mean total cell fluorescence (Tables S2 and S3).

We calculated the numbers of molecules in a patch from the mean fluorescence intensity in a six-pixel wide circular area containing the patch minus the mean cytoplasmic fluorescence. We converted fluorescence intensities to molecules using the whole cell calibration curve followed by a correction by a factor of 0.00887 to account for the ratio of patch area to whole cell area. Numbers of molecules calculated from time series were corrected for the photobleaching using rates determined by fitting single exponentials to time series of background-corrected and averaged mean fluorescence intensities of whole cells.

We measured time courses for 6–15 individual patches for each GFP- or YFP-labeled protein. For each patch, we recorded the time points when a patch appeared, initiated movement, reached the peak number of molecules and disappeared and then calculated time intervals between these events (Table 1 and Table S2). Maximum number of molecules and total distance moved were averaged for all patches tracked with a particular protein (Table 1 and Table S2). To produce average time courses we selected 3–7 representative time courses (that showed the same variation as the rest of the data), aligned these time courses, except clathrin and Myo1p, to the time when each patch moved (time 0), and averaged the number of molecules at each time point. For averaging, we aligned clathrin time courses to the time of disappearance of clathrin from patches and Myo1p time courses to the time of the Wsp1p peak. The peak number of molecules calculated from averaged time courses is slightly smaller than the maximum number shown in Table 1 and Table S2 due to variation in timing of the peak.

RESULTS

Tagging Endocytic Actin Patch Components with Fluorescent Proteins

We tagged 16 fission yeast proteins known to be involved in endocytosis or actin assembly with green fluorescent protein or its spectral variants YFP and CFP (Table S1). Myosin-1 (Myo1p), Wiskott-Aldrich syndrome protein (Wsp1p) and actin (Act1p) were tagged on their N-termini. All other proteins were tagged at their C-termini. All genes were tagged directly in the genome and expressed from native chromosomal locations and, except actin, under the control of native promoters. In haploid strains each tagged protein was the only source of a given gene product.

We determined whether the proteins tagged with fluorescent proteins were functional in haploid strains using four tests: 1) cell morphology by DIC microscopy; 2) growth rates at 25 and 36°C; 3) growth and colony formation under stress conditions (36°C or 1 M KCl); and 4) genetic crosses with a myosin-1 gene deletion (Δ*myo1*) strain to check for synthetic lethality. By these criteria, 11 of the tagged proteins were fully functional (Table 1; Table S2). In spite of fulfilling three of these criteria, tagged Wsp1p and three subunits of Arp2/3 complex (Arp2, Arp3, and ARPC5) could not be combined with Δ*myo1*. The synthetic lethality of the mGFP-Wsp1p and ARPC5-mGFP with Δ*myo1* may be due to loss of function specifically during mating and sporulation, because mGFP-Wsp1p and ARPC5-mGFP could be combined with a *myo1* shut-off strain that allowed myosin-1 expression during mating and sporulation. Immunoblots of cell extracts with antibodies to fluorescent protein verified that the tagged proteins (except Pan1p) were intact.

GFP-tagged actin cannot replace native actin, because fission yeast do not incorporate GFP-actin into actin cables or contractile rings dependent on formins (Wu and Pollard, 2005; Wu *et al.*, 2006), so we used a heterozygous *mGFP-act1/act1*$^+$ diploid strain with one actin gene tagged with GFP on the N-terminus and expressed from native locus but under control of the *nmt1* promoter. These diploid cells produced ~2 μM GFP-actin (Table S3), and quantitative immunoblots verified half as much native actin as in wild-type diploid cells. Given that diploids are about twice the size of haploids, the concentration of untagged actin was ~32 μM, half that of haploids (Wu and Pollard, 2005). Hence, GFP-actin constituted ~6% of total actin, which is similar to ~10% measured by immunoblotting. GFP-actin expressed in this diploid strain incorporated into actin patches (see below); however, upon sporulation of the *mGFP-act1/act1*$^+$ strain, we were unable to recover haploid cells expressing GFP-actin as the sole actin source, and such cells failed to germinate or divide.

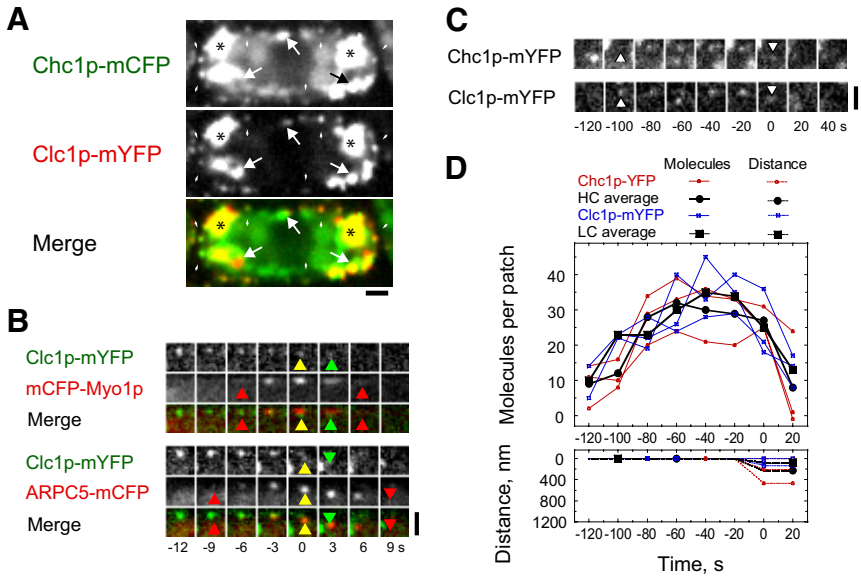

Figure 2. Time course of clathrin accumulation and loss in endocytic actin patches in spinning disk confocal fluorescence micrographs. (A) Images through the midsection of a cell showing Chc1p-mCFP (green) and Clc1p-mYFP (red) in two types of structures: dim peripheral patches (arrowheads) and bright intracellular globular structures (arrows and asterisks) of two different sizes. (B) Images through the midsection of cells showing one-to-one transitions of patches marked with clathrin (Clc1p-mYFP top rows, green in merge) into patches marked with Myo1p or Arp2/3 complex (mCFP-Myo1p or ARPC5-mCFP, middle rows, red in merge). Green arrowheads mark the last frames where Clc1p is present, red arrowheads mark the first and last frames where Myo1p and Arp2/3 complex were present, and yellow arrowhead marks initiation of patch movement. (C) Images through the midsections of cells showing individual patches marked with Chc1p-mYFP or Clc1p-mYFP. Note that clathrin moved in the last frame where the patch was present (arrowhead). (D) Raw and average time courses for YFP-labeled clathrin heavy-chain Chc1p and clathrin light-chain Clc1p. Raw time courses for three Chc1p-mYFP (red, ○) and three Clc1p-mYFP (blue, □) patches were aligned to the time of disappearance of clathrin at +20 s and averaged to produce time courses for the average numbers of clathrin heavy chains (black, ●) and clathrin light chains (black, ■) per patch (top panels, solid lines) and distances traveled by clathrin associated with patches (bottom panels, dashed lines).

Validation of Methods Used to Measure Protein Numbers Over Time

The intensity of YFP or GFP fluorescence detected by microscopy is directly proportional to the number of fluorescent protein molecules (Wu and Pollard, 2005), so we used fluorescence intensity to measure the cytoplasmic concentrations of the tagged proteins in interphase cells and protein numbers in actin patches (Table 1, Tables S2 and S3). To track protein numbers in actin patches over time (Figures 1 and 2; see also Figures 4–7), we optimized image acquisition, improved methods to correct for cytoplasmic background and photobleaching, and developed a strategy for aligning data on the same time scale.

Image Acquisition. We used different methods for fusion proteins tagged with GFP and YFP (Figure 1): 1) 3D method with GFP: Except for clathrin, the fluorescence from GFP fusion proteins was sufficiently bright and stable to record stacks of sections in 0.6-μm steps through the full thickness of cells as frequently as every 2–3 s for 40–60 s. Generally, three consecutive optical sections spanning 1.2 μm contained the entire fluorescent signal from each patch. 2) 2D method with YFP: YFP photobleaches faster than GFP, so we recorded the fluorescence in a single confocal section of cells every 2–3 s. Z-series established that a single confocal section through the midsection of a cell contained 11% of the total cell fluorescence and 51% of total patch fluorescence for those patches in sharp focus in the middle section. We made our YFP measurements on sharply focused patches and assumed that they contained 51% of each protein in the patch. With this correction, numbers measured by the two strategies with either GFP or YFP agreed remarkably well (Tables S2 and S3; Figure 1; see also Figures 4–6).

Correction for Cytoplasmic Background. Proteins in the soluble cytoplasmic pool are expected to penetrate the filament network in patches, so we subtracted their fluorescence value from the intensity of patches to obtain the number of molecules immobilized in patches. We measured cytoplasmic background fluorescence corresponding to the pool of free proteins in carefully selected areas away from patches, nuclei, and vacuoles (Figure 1B). Cytoplasmic background measured in this way was lower than the background measured in the area immediately surrounding each patch (Wu and Pollard, 2005), which may include fluorescence from adjacent patches. Consequently, the numbers of molecules in patches measured with our method were about twofold higher than with the Wu and Pollard method (Table 1; Tables S2 and S3; Figure S1), which is better suited for measurements of well-separated structures such as contractile rings or spindle pole bodies than actin patches.

Correction for Photobleaching. Acquisition parameters were such that fluorescence declined exponentially by ~40% over 60 s during image acquisition at 3-s intervals for both single sections with YFP and Z-stacks with GFP. We measured photobleaching rate constants in each experiment and corrected the intensity of the images before calculating numbers of molecules at each time point.

Timing. We put all of our temporal measurements on the same absolute time scale using as time 0 the time that patches started to move from the surface, which we assume coincided with endocytic internalization (Figures 1 and 2; see also Figures 4–7). This is possible, because all markers except Myo1p were present together for the first few seconds that patches moved. Because Myo1p patches did not move, we aligned Myo1p traces on the time scale using the observation that Myo1p peaks at the same time as Wsp1p (Sirotkin *et al.*, 2005).

We verified the order of appearance of patch components using strains expressing the two proteins tagged with YFP and CFP (Table S4; Figure S2). Of all the tagged proteins, only tags on Arp2/3 complex subunits changed patch dynamics. To compensate for the slower reactions, we adjusted the time courses for Arp2/3 complex so that it matched the time course of fimbrin (see below). The corrected time course restored the correct order of assembly of actin patch components, observed by two-color imaging.

Quantitation of Actin Patch Assembly and Disassembly

Each of the 16 tagged proteins concentrated in endocytic actin patches in a defined order with strictly controlled timing (Table 1; Table S2; see also Figures 1–7). Clathrin light chains and heavy chains appeared at about −100 s (Figure 2), followed by adapter proteins End4p and Pan1p at −36 to −32 s (see Figure 4), three activators of Arp2/3 complex (Myo1p, Wsp1p and Vrp1p) at −12 to −9 s followed 2 s later by Arp2/3 complex (see Figure 5). Actin, capping protein, fimbrin, and other actin-binding proteins except coronin, closely followed Arp2/3 complex (see Figure 6).

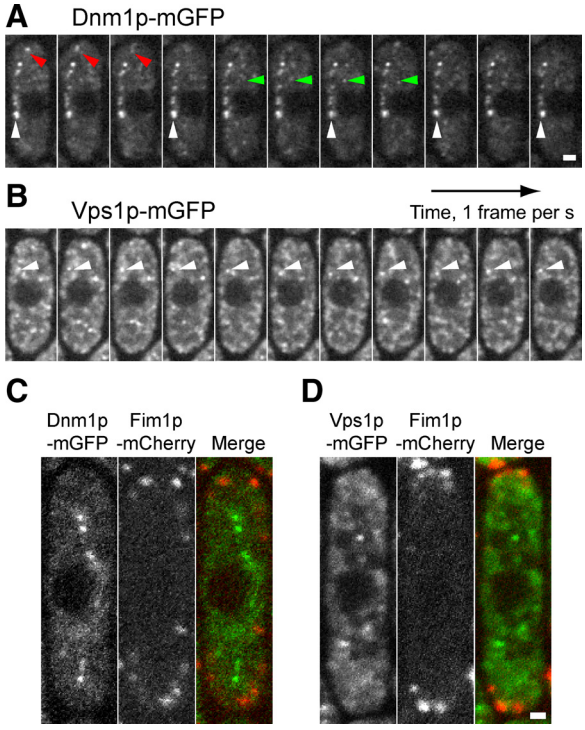

Figure 3. Localization and dynamics of mGFP-tagged dynamin-like proteins in fission yeast. (A and B) Time series of spinning disk confocal fluorescence micrographs acquired every second through the middle of cells expressing (A) Dnm1p-mGFP and (B) Vps1p-mGFP. Dynamin Dnm1p concentrates in punctate structures that form linear arrays (white arrowheads) or move in/out of focus (green/red arrowheads). Vps1p is detected in reticulate meshwork throughout the cytoplasm and in small motile dots (arrowheads). (C and D) Comparison of localization of dynamin-like proteins with actin patch marker fimbrin Fim1p in single confocal sections through the middle of the cells expressing (C) Dnm1p-mGFP (green in merge) and Fim1p-mCherry (red in merge) or (D) Vps1p-mGFP (green in merge) and Fim1p-mCherry (red in merge). Note the complete lack of colocalization. Scale bars, 1 μm.

Each protein reached a characteristic peak at a specific time (see Figure 7): clathrin light and heavy chains have a broad peak from −90 to 0 s, followed by sharper peaks for Arp2/3 complex activators at −3 to −2 s, Arp2/3 complex, actin and actin-binding proteins (except coronin) at time 0, and coronin at +5 s. During patch movement, clathrin and Arp2/3 complex activators rapidly dissipated from patches in 3–6 s, whereas endocytic adaptors and components of actin network gradually dissociated over the course of 9–15 s. The examples in Figures 1 and 2 (see also Figures 4–6) show that the peak numbers of molecules are reproducible within 30–50% from patch to patch. The following sections elaborate on key features of these time courses. The accompanying article by Berro *et al.* (2010) presents computer simulations of mathematical models to provide a quantitative basis for interpreting the mechanistic implications of the timing and number of participating molecules.

Assembly of Clathrin Precursors of Endocytic Actin Patches

Clathrin heavy and light chains concentrated together in three structures: large, mobile globular structures, small highly mobile cytoplasmic puncta, and cortical patches (Figure 2A). The globular structures and puncta, which likely represent membrane-sorting compartments (Newpher *et al.*, 2005), often obscured clathrin associated with cortical patches. Of the ~52,000 clathrin heavy chains and ~36,000 light chains in an average fission yeast cell, 25–30% were free in the diffuse cytoplasmic pool at a concentration of ~0.8 μM for the heavy chains (Table 1).

Clathrin accumulated in cortical patches over ~20–40 s to an average of ~30 and a maximum of ~40 heavy chains and light chains for the 70–115-s lifetimes of the patches (Table 1; Table S2; Figure 2D). Clathrin patches were immobile until time 0, when they moved <0.5 μm from the plasma membrane over ~3–6 s as they faded in intensity (Figure 2, B and C). Of 48 patches marked with YFP-labeled clathrin, 46 (96%) acquired CFP-labeled Arp2/3 complex more than a minute later. Similarly, 82–91% of YFP-labeled clathrin patches acquired CFP-tagged Pan1p, Myo1p, and Crn1p after delays of 60–80 s.

Fission Yeast Endocytosis Does Not Involve Dynamin

S. pombe has genes for three proteins related to dynamin (Dnm1p, Vps1p, and Msp1p), but none of these proteins appear to participate in endocytosis. Guillou *et al.* (2005) reported that Msp1p localizes to mitochondria. We tagged the other two fission yeast dynamin-like proteins with mGFP at the C-terminus and detected no Dnm1p-mGFP or Vps1p-mGFP in actin patches (Figure 3). Dnm1p-mGFP concentrated in punctate intracellular structures, often organized in linear arrays (Figure 3A). Vps1p-mGFP distributed throughout the cytoplasm and concentrated in small dynamic aggregates of unknown nature (Figure 3B). No Dnm1p-mGFP or Vps1p-mGFP concentrated in actin patches labeled with Fim1p-mCherry in time-lapse movies or in single confocal sections, which contained patches at random points in their lifetimes (Figure 3, C and D). In agreement with localization data, patch dynamics are normal in Δvps1 deletion strains (Arasada, R., and Pollard, T. D., unpublished data). Instead, recent studies reported roles for Vps1p and Dnm1p in peroxisome, mitochondria, and vacuole biogenesis (Jourdain *et al.*, 2008, 2009; Rothlisberger *et al.*, 2009).

Assembly of Endocytic Adaptors, Arp2/3 Complex Activators, and Arp2/3 Complex

The endocytic adaptor proteins End4p (Sla2p in budding yeast) and Pan1p concentrated with clathrin before the actin machinery and reached peak numbers of molecules along with Arp2/3 complex at time 0 (Figure 4 and see also Figure

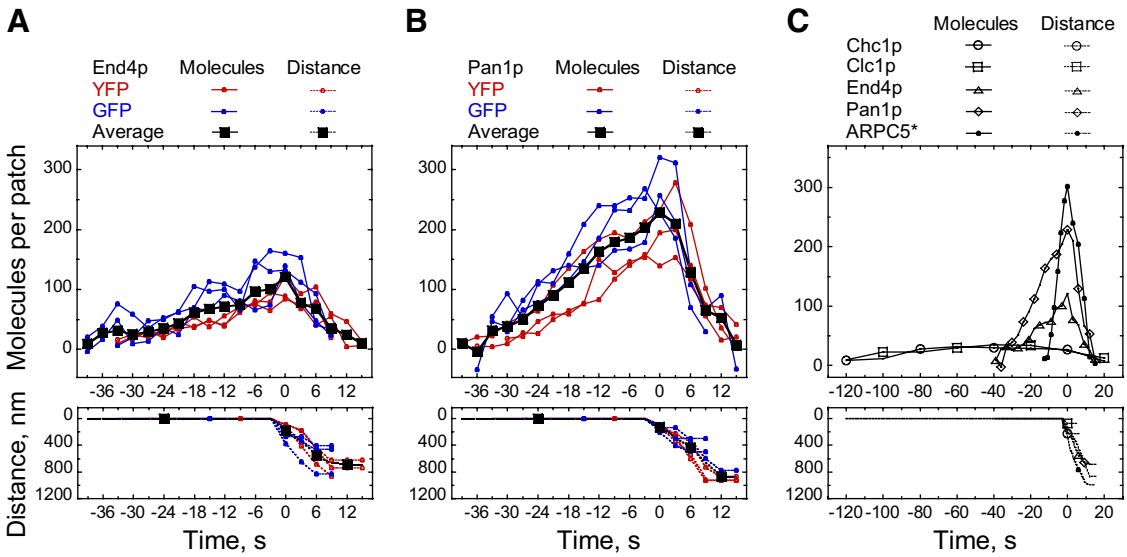

Figure 4. Time courses of the concentrations of endocytic adaptor proteins End4p and Pan1p in endocytic patches. (A and B) Raw and average time courses of the number of molecules per patch (top panels, solid lines) and distances traveled by markers associated with patches (bottom panels, dashed lines). (A) End4p. (B) Pan1p. Time courses for YFP-labeled (red, ○) and GFP-labeled (blue, ●) proteins in individual patches were aligned to initiation of patch movement at time 0 and averaged at each time point to produce averaged time courses (black, ■). Numbers of GFP-labeled proteins were calculated from time-lapse movies of Z-sections through entire cells. Numbers of YFP-labeled proteins were calculated from time-lapse movies in single sections through the middle of cells. Averages include data from three YFP-labeled and three GFP-labeled patches. (C) Comparison of average time courses for (○) clathrin heavy-chain Chc1p, (□) clathrin light-chain Clc1p, (△) End4p, (◇) Pan1p, and (●) ARPC5 subunit of Arp2/3 complex. Time courses were aligned to the initiation of patch movement (time 0). The Arp2/3 complex time course was corrected (∗) to match the timing of patch assembly of fimbrin.

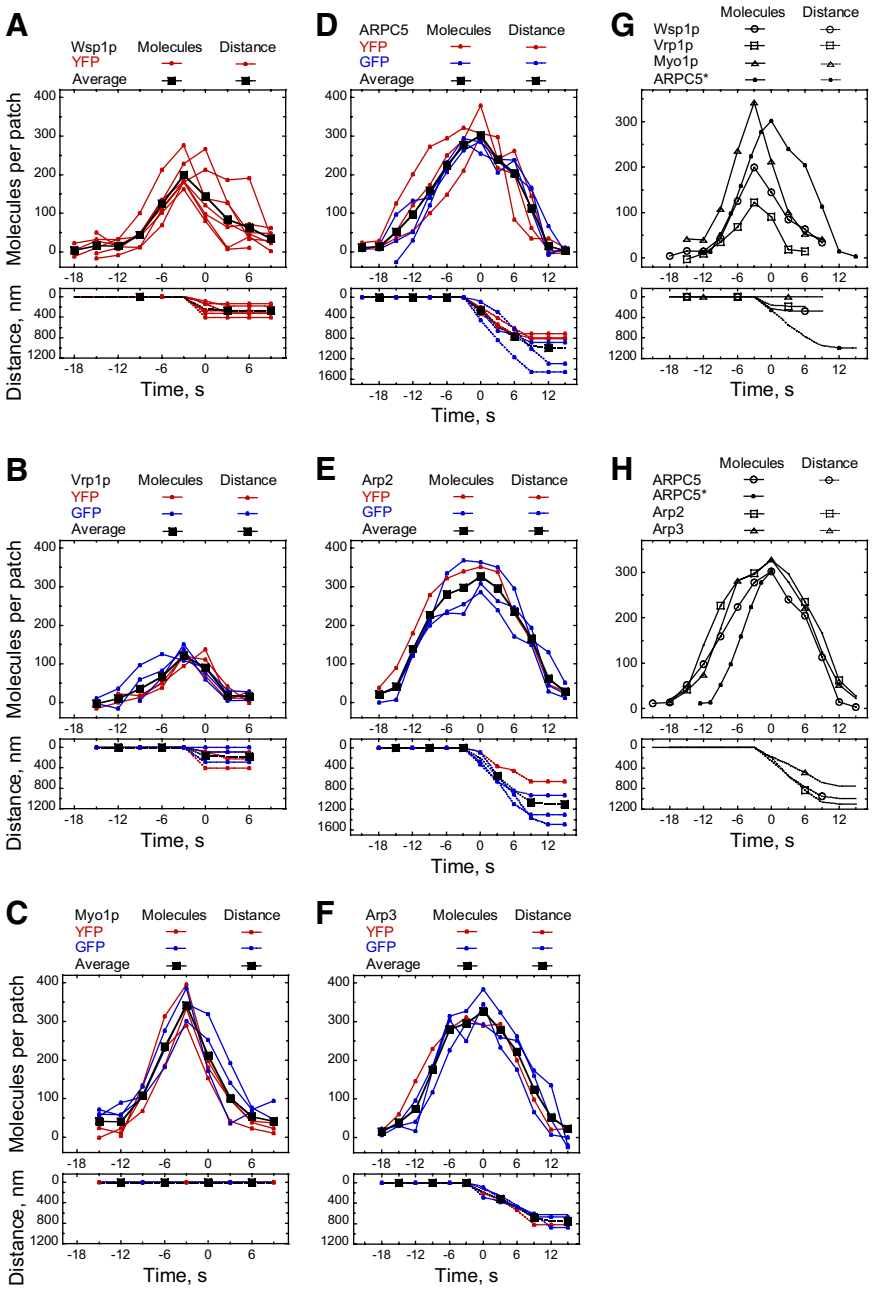

Figure 5. Time courses of the concentrations of Arp2/3 complex activators Wsp1p, Vrp1p, and Myo1p and Arp2/3 complex subunits ARPC5, Arp2, and Arp3 in endocytic patches. (A–F) Raw and average time courses of the number of molecules per patch (top panels, solid lines) and distances traveled by markers associated with patches (bottom panels, dashed lines). (A) WASp Wsp1p. (B) Verprolin Vrp1p. (C) Myosin-1 Myo1p. (D) ARPC5. (E) Arp2. (F) Arp3. Time courses for YFP-labeled (red, ○) and GFP-labeled (blue, ●) proteins in individual patches were aligned and averaged at each time point to produce averaged time courses (black, ■). Time courses were aligned to initiation of patch movement at time 0, except for the time courses for Myo1p, which were aligned to peak values. Numbers of GFP-labeled proteins were calculated from time-lapse movies of Z-sections through entire cells. Numbers of YFP-labeled proteins were calculated from time-lapse movies in single sections through the middle of cells. Averages include data from seven YFP-labeled patches for Wsp1p, and one YFP- and three GFP-labeled patches for Arp2 and Arp3, and three YFP- and three GFP-labeled patches for all others. (G and H) Comparison of average time courses for Arp2/3 complex activators and subunits of Arp2/3 complex. (G) Average time courses for (○) Wsp1p, (□) Vrp1p, (△) Myo1p, and (●) ARPC5 subunit of Arp2/3 complex. (H) Average time courses for (○) ARPC5, (□) Arp2, (△) Arp3 subunits of Arp2/3 complex and (●) adjusted time course for the ARPC5 subunit. Time courses were aligned to the initiation of patch movement (time 0), and peak of Myo1p time course was aligned to the time of Wsp1p peak. Asterisk (*) indicates that the (●) ARPC5* time course was corrected to match the timing of assembly of fimbrin into patches.

7). End4p accumulated in two phases: ~30 molecules of End4p appeared at −36 s, plateaued for ~9 s, and then additional 90 End4p molecules accumulated over the following 24–27 s. The 230 molecules of Pan1p accumulated at a steady rate starting from −33 s.

Arp2/3 complex activators appeared at about −10 s and reached peaks of 340 Myo1p, 200 Wsp1p, and 120 Vrp1p molecules at −2 to −3 s, preceding the peak of Arp2/3 complex at time 0 (Figure 5; see also Figure 7). Each patch accumulated a characteristic peak number of 300–330 Arp2, Arp3, and ARPC5 subunits of Arp2/3 complex (Figure 5). The appearance of Arp2/3 complex labeled with fluorescent proteins at 13–19 s before the patches moved (Table 1; Table S2; Figures 1 and 5) gave the impression that Arp2/3 complex preceded Wsp1p and Myo1p. However, imaging cells with contrasting fluorescent protein tags on Arp2/3 complex and either Wsp1p, Myo1p, fimbrin, or capping protein showed that Wsp1p and Myo1p actually appeared several seconds before Arp2/3 complex (Sirotkin *et al.*, 2005) and that a fluorescent protein tag on the ARPC5 slowed the accumulation of fimbrin and capping protein and onset of movement of the whole patch (Table S4; Figure S2). Because tagged subunits of Arp2/3 complex and tagged fimbrin assembled together, we adjusted timing of Arp2/3 complex assembly into patches (see Figures 4–7) to match that of fimbrin Fim1p (Figure 6A).

Assembly of Actin and Actin-binding Proteins

We estimated the concentration of actin in patches by measuring the concentration of GFP-actin in heterozygous *mGFP-act1/act1*$^+$ diploid cells. These mutants expressed half the normal level of unlabeled actin (32 μM) and 2 μM

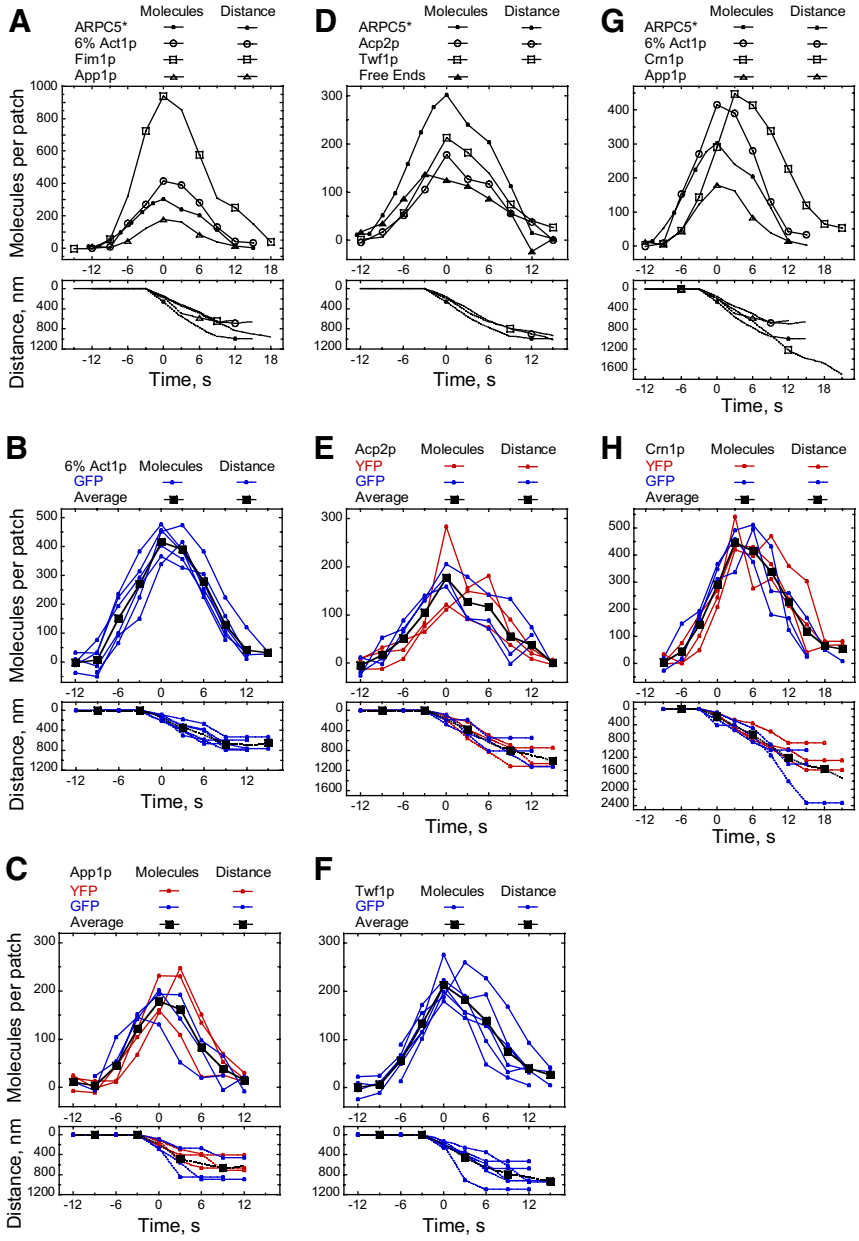

Figure 6. Time courses of the concentrations of actin and actin-binding proteins in endocytic patches. Comparison of raw and average time courses of the number of molecules per patch (solid lines, top panels) and distance traveled by patches (dashed lines, bottom panels) for Arp2/3 complex, actin and actin-binding proteins. (A–C) Time courses for actin Act1p, fimbrin Fim1p, and App1p. (A) Comparison of average time courses for (○) mGFP-Act1p estimated to represent 6% of total actin, (□) fimbrin Fim1p, and (△) App1p versus (●) ARPC5* time course that was corrected to match the timing of assembly of fimbrin into patches. (B and C) Raw and average time courses. (B) mGFP-Act1p. (C) App1p. (D–F) Time courses for actin-capping protein Acp2p and twinfilin Twf1p. (D) Comparison of (●) adjusted average ARPC5* time course with average time courses for (○) capping protein Acp2p, (□) twinfilin Twf1p, and (▲) the maximum number of growing barbed actin filament ends. The maximum number of growing ends is the difference between the number of ARPC5 and Acp2p molecules. (E and F) Raw and average time courses. (E) Acp2p. (F) Twf1p. (G and H) Time courses for coronin Crn1p. (G) Comparison of (●) adjusted average ARPC5* time course with average time courses for (○) mGFP-Act1p estimated to represent 6% of total actin, (□) coronin Crn1p, and (△) Abp1p homolog App1p. Note that Crn1p appears and peaks 3–5 s after the other proteins. (H) Raw and average time courses for Crn1p. In B, C, E, F, and H, raw time courses for YFP-labeled (red, ○) and GFP-labeled proteins (blue, ●) in individual patches were aligned to the time of initiation of patch movement at time 0 and the molecules per patch (top panels, solid lines) and distance (bottom panels, dashed line) traveled by markers associated with patches were averaged at each time point to produce average time courses (black, ■). Numbers of GFP-labeled proteins were calculated from time-lapse movies of Z-sections through entire cells. Numbers of YFP-labeled proteins were calculated from time-lapse movies in single sections through the middle of cells. Averages include data from six GFP-labeled patches for Act1p and Twf1p, and three YFP- and three GFP-labeled patches for all others.

mGFP-actin (6% of total) and accumulated GFP-actin in patches over 7–9 s to a peak of ~415–450 molecules, corresponding to ~7000 total actin molecules (Table 1; Table S2; Figures 6 and 7). The accompanying article (Berro *et al.*, 2010) considers the consequences of the higher concentration of actin in wild-type haploid cells in modeling the assembly of actin patches.

The actin filament–binding proteins fimbrin (Fim1p), App1p, twinfilin (Twf1p), and capping protein (Acp2p) accumulated in stationary patches over the same time course as actin (Table 1; Table S2; Figures 6 and 7). By time 0, each patch accumulated a characteristic peak number of actin-binding proteins: ~300 molecules of Arp2/3 complex, ~900 molecules of Fim1p, and ~200 molecules of Acp2p, Twf1p, and App1p. The peak of ~450–500 coronin molecules trailed actin and the other actin-binding proteins by 3–5 s (Table 1; Tables S2 and S4; Figures 1, 6, and 7; Figure S2). Starting at time 0, Arp2/3 complex, actin, and all of the actin-binding proteins in a patch moved away from the plasma membrane by up to 1.6 μm over ~9–15 s. As the patch moved, the numbers of all proteins declined down to zero. Coronin lagged behind the other proteins by a few seconds, but never persisted for minutes or moved several micrometers as described previously (Pelham and Chang, 2001).

DISCUSSION

Quantitative confocal microscopy showed that fission yeast cells strictly control both timing and the numbers of molecules that appear and disappear over time at sites of endocytosis, starting with a hemisphere of clathrin and culminating in a wave of actin assembly (Kaksonen *et al.*, 2003, 2005; Sirotkin *et al.*, 2005). This reproducibility makes yeast advantageous for studying the role of actin assembly in clathrin-mediated endocytosis.

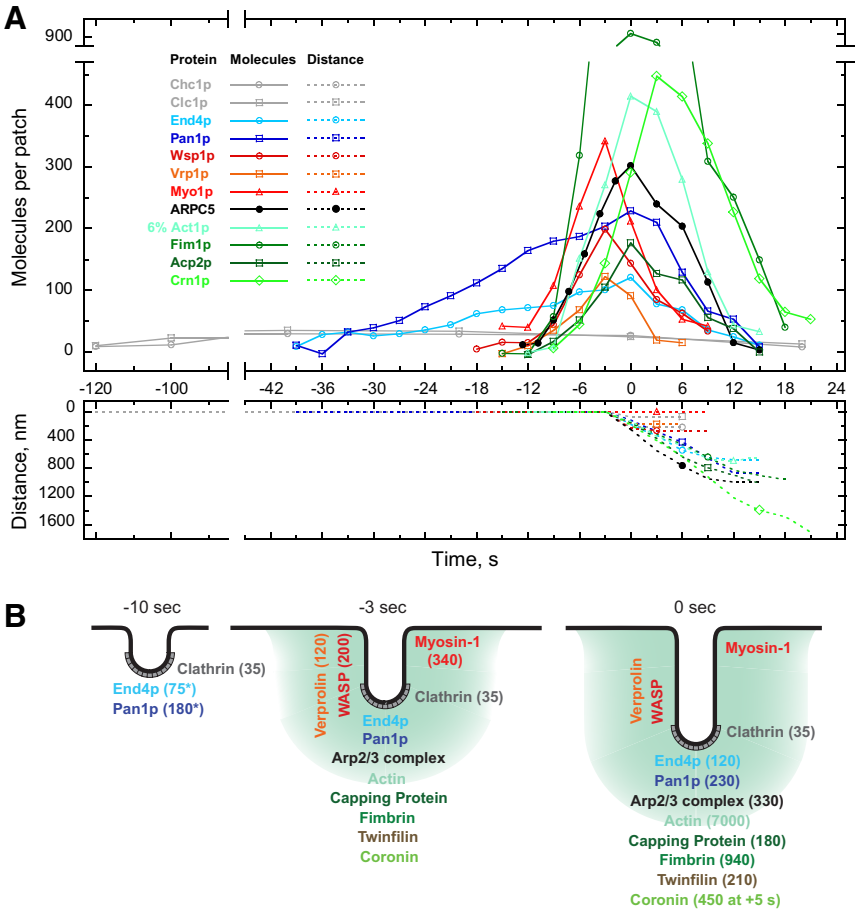

Figure 7. Summary time course of the assembly and disassembly of actin patch proteins at the site of endocytosis. (A) Summary time course of the number of molecules (solid lines) and distance traveled (dashed lines) of 12 endocytic actin patch components. Each time course is an average of data for three YFP-labeled patches for clathrin, seven YFP-labeled patches for Wsp1p, six GFP-labeled patches for Act1p, and three YFP- and three GFP-labeled patches for all other components. Numbers of GFP-labeled proteins were calculated from time-lapse 3D image series and numbers of YFP-labeled proteins were calculated from time-lapse series in one confocal section. All time courses were aligned to time 0, which marks initiation of patch movement, except for Myo1p, which was aligned with the Wsp1p peak. The ARPC5 time course was corrected so that the timing of patch assembly matched that of fimbrin. mGFP-Act1p is estimated to represent 6% of total actin. (B) Schematic diagram illustrating counts of proteins associated with an actin patch at the site of endocytic invagination at times −10, −3, and 0 s. Colors of fonts correspond to the colors in A. Numbers in parenthesis indicate the peak numbers of each protein, except for End4p and Pan1p at −10 s (asterisks). All of the proteins listed below Arp2/3 complex are presumed to be distributed throughout the actin network (shaded teal). The approximate positions of other proteins are adapted from Idrissi *et al.* (2008).

Recruitment of Clathrin

In response to unknown stimuli fission yeast cells assemble clathrin in patches 1–2 min before Arp2/3 complex appears. The ~30–40 clathrin molecules in patches suffice to assemble a hemisphere rather than a full barrel cage consisting of 108 clathrin molecules in 36 triskelions (Fotin *et al.*, 2004). Clathrin likely coats just the rounded tip of the finger-like invagination of the plasma membrane as observed by EM in budding yeast (Mulholland *et al.*, 1994; Idrissi *et al.*, 2008) and proposed by Kirchhausen (2009). A hemisphere of clathrin is expected to have a maximum diameter of ~70 nm, large enough to coat the 50-nm vesicles inside filasomes, putative actin patch structures identified by electron microscopy of fission yeast (Kanbe *et al.*, 1989; Takagi *et al.*, 2003). Factors other than clathrin must contribute to marking the endocytic site, because actin patches still form and internalize slowly in the absence of clathrin (Kaksonen *et al.*, 2005; Newpher and Lemmon, 2006). These additional factors include Ede1p and Syp1p in budding yeast (Reider *et al.*, 2009; Stimpson *et al.*, 2009) and FCHo1/2, eps15, and intersectin in animals (Henne *et al.*, 2010).

Role of Dynamin

As in budding yeast (Praefcke and McMahon, 2004), the GTPase dynamin does not participate in clathrin-dependent endocytosis in fission yeast. Although clathrin-mediated endocytosis in animal cells usually depends on dynamin, animal cells lacking dynamin accumulate tubular endocytic invaginations similar to those in yeast, including dependence on actin assembly (Ferguson *et al.*, 2009). Therefore, animal cells retain from their common ancestor with fungi the capacity to use actin assembly for internalization of endocytic vesicles.

Recruitment of Endocytic Adaptors

The reactions linking clathrin to endocytic adaptors and nucleation-promoting factors for Arp2/3 complex are the least understood steps in the pathway. Given the stoichiometry and timing (Figures 4 and 7), End4p and Pan1p must interact with a succession of ligands at sites of endocytosis, and our quantitative data on the accumulation and loss of End4p and Pan1p put strong constraints on the underlying reactions. We interpret the initial accumulation of 30 End4p molecules at −33–36 s to represent 1:1 binding to clathrin light chains (Newpher *et al.*, 2006). Given that ~1 μM cytoplasmic End4p saturates the patch binding sites in 3 s, the K_d is <1 μM, the association rate constant is >0.3 μM^{-1} s^{-1}, and the dissociation rate is <0.3 s^{-1}. The trigger for the onset of this favorable reaction with a remarkable delay of 40–80 s after assembly of clathrin is unknown. Although initial recruitment of ~30 Pan1p molecules at −33 s may depend on interaction with End4p (Toshima *et al.*, 2007), subsequent accumulation of additional 90 End4p molecules and 200 Pan1 molecules over 24–27 s may be mediated by multiple interactions among endocytic adaptors. For example, Pan1p can bind Ent1/2p, End3p, Sla2p/End4p, and Sla1p (Toshima *et al.*, 2007), all of which are present in fission yeast. Interactions with phosphatidylinositol-4,5-bisphosphate (PIP_2) may limit the recruitment of adaptors. PIP_2 accumulates in budding yeast patches in parallel with Sla2p

(Sun *et al.*, 2007), and patch dynamics depend on interaction of Sla2p with PIP_2 (Sun *et al.*, 2007).

Recruitment of Arp2/3 Complex Activators

Timing, biochemical analysis, and effect of mutations suggest that Wsp1p is the primary activator of Arp2/3 complex in patches in budding and fission yeast (Sirotkin *et al.*, 2005; Sun *et al.*, 2006; Galletta *et al.*, 2008), but myosin-1 Myo1p and Pan1p can activate Arp2/3 complex in the absence of Wsp1p and are likely to contribute to Arp2/3 complex activation in the presence of Wsp1p (Sun *et al.*, 2006; Galletta *et al.*, 2008). Wsp1p also recruits verprolin (Vrp1p) to patches (Sirotkin *et al.*, 2005) in excess of their ratio in cytoplasm (Table 1; Table S2). Vrp1p may regulate Wsp1p like other WASp family members (Ho *et al.*, 2004) and also interacts with Myo1p (Sirotkin *et al.*, 2005). Myo1p near the base of plasma membrane invaginations (Idrissi *et al.*, 2008) may activate a spatially restricted population of Arp2/3 complex. What triggers the initial recruitment and activation of Wsp1p and Myo1p is unknown. The weakest of the three known activators, Pan1p, arrives in patches well before Arp2/3 complex (Figure 7) and may initiate the first actin filaments.

Actin Patch Assembly

In the accompanying article Berro *et al.* (2010) used the quantitative kinetic data in this article to formulate and test a mathematical model of actin filament assembly and disassembly. This analysis supports the general features of the dendritic nucleation hypothesis and also provides a rare estimate of reaction rates inside cells.

The simulations show that patches form ~150 actin filament branches that grow 100–200 nm long before being capped rapidly, so that fewer than 10 barbed ends are growing at any point in time. Two bimolecular reactions, actin filament capping and Arp2/3 complex binding to the sides of actin filaments, are faster in the cell than in vitro. Excluded volume effects, geometry, or additional protein factors, such as F-BAR protein Bzz1p (Arasada, R., and Pollard, T. D., unpublished data) may contribute to the higher rate of branching in cells.

Actin patches contain a maximum of ~900 fimbrin molecules, sufficient to cross-link each short filament several times, if each fimbrin binds two filaments. Such cross-linked filament networks may provide mechanical support for membrane invagination and scission, explaining why in the absence of fimbrin patches fail to internalize (Kaksonen *et al.*, 2005).

Actin Patch Disassembly

During patch internalization, Myo1p stays behind on the membrane, whereas all other components move together as a single unit but dissociate from patches at characteristic times (Figure 7). Clathrin and Wsp1p/Vrp1p leave first, followed by End4p, Pan1p, actin, and all actin-binding proteins, except coronin, which arrives last and persists in patches the longest.

Our quantitative data and computer simulations can explain the rapid disappearance of actin in 10 s only if the filaments are severed into short fragments that diffuse away in addition to subunit dissociation from filament ends. This mechanism is consistent with our observation that actin, Arp2/3 complex and capping protein disappear from patches with similar kinetics despite vastly different rates of dissociation from filaments in vitro. Budding yeast actin patches recruit cofilin, Aip1p, and coronin (Okreglak and Drubin, 2007, 2010; Lin *et al.*, 2010) with kinetics similar to coronin in fission yeast, so the three proteins may cooperate in patch disassembly (Humphries *et al.*, 2002; Brieher *et al.*, 2006; Gandhi *et al.*, 2009). Given the excess of coronin over Arp2/3 complex, most of the coronin is likely bound to actin filaments.

Overview of Current Knowledge

Mathematical modeling shows that the remarkable control of the number of molecules at endocytic sites may be achieved by self-assembly at a limited number of binding sites as determined by the stoichiometry and kinetics of interacting proteins. However, the effects of mutations and actin-disrupting drugs (Kaksonen *et al.*, 2006) suggest that feedback mechanisms may regulate some of the steps, for example, recruitment of endocytic adaptors and Arp2/3 complex activators via yet to be discovered mechanisms.

ACKNOWLEDGMENTS

We are grateful to our laboratory colleagues Drs. J.-Q. Wu, D. Kovar, C. Beltzner, and J. Kuhn for strains and technical advice and to Dr. K. Sawin (University of Edinburgh) for mCherry tagging cassette. This work was supported by National Institutes of Health Grants GM-026132 and GM-0026338 to T.D.P., an American Heart Association postdoctoral fellowship 022579T to V.S., and an EMBO postdoctoral fellowship ALTF 1261-2007 to J.B.

REFERENCES

Bahler, J., Wu, J. Q., Longtine, M. S., Shah, N. G., McKenzie, A., 3rd, Steever, A. B., Wach, A., Philippsen, P., and Pringle, J. R. (1998). Heterologous modules for efficient and versatile PCR-based gene targeting in *Schizosaccharomyces pombe*. Yeast *14*, 943–951.

Berro, J., Sirotkin, V., and Pollard, T. D. (2010). Mathematical modeling of endocytic actin patch kinetics in fission yeast: disassembly requires release of actin filament fragments. Mol. Biol. Cell *21*, 2905–2915.

Brieher, W. M., Kueh, H. Y., Ballif, B. A., and Mitchison, T. J. (2006). Rapid actin monomer-insensitive depolymerization of *Listeria* actin comet tails by cofilin, coronin, and Aip1. J. Cell Biol. *175*, 315–324.

Ferguson, S. M., *et al.* (2009). Coordinated actions of actin and BAR proteins upstream of dynamin at endocytic clathrin-coated pits. Dev. Cell *17*, 811–822.

Fotin, A., Cheng, Y., Sliz, P., Grigorieff, N., Harrison, S. C., Kirchhausen, T., and Walz, T. (2004). Molecular model for a complete clathrin lattice from electron cryomicroscopy. Nature *432*, 573–579.

Galletta, B. J., Chuang, D. Y., and Cooper, J. A. (2008). Distinct roles for arp2/3 regulators in actin assembly and endocytosis. PLoS Biol *6*, e1.

Galletta, B. J., and Cooper, J. A. (2009). Actin and endocytosis: mechanisms and phylogeny. Curr. Opin. Cell Biol. *21*, 20–27.

Gandhi, M., Achard, V., Blanchoin, L., and Goode, B. L. (2009). Coronin switches roles in actin disassembly depending on the nucleotide state of actin. Mol. Cell *34*, 364–374.

Guillou, E., Bousquet, C., Daloyau, M., Emorine, L. J., and Belenguer, P. (2005). Msp1p is an intermembrane space dynamin-related protein that mediates mitochondrial fusion in a Dnm1p-dependent manner in *S. pombe*. FEBS Lett. *579*, 1109–1116.

Henne, W. M., Boucrot, E., Meinecke, M., Evergren, E., Vallis, Y., Mittal, R., and McMahon, H. T. (2010). FCHo proteins are nucleators of clathrin-mediated endocytosis. Science *328*, 1281–1284.

Ho, H. Y., Rohatgi, R., Lebensohn, A. M., Le, M., Li, J., Gygi, S. P., and Kirschner, M. W. (2004). Toca-1 mediates Cdc42-dependent actin nucleation by activating the N-WASP-WIP complex. Cell *118*, 203–216.

Huckaba, T. M., Gay, A. C., Pantalena, L. F., Yang, H. C., and Pon, L. A. (2004). Live cell imaging of the assembly, disassembly, and actin cable-dependent movement of endosomes and actin patches in the budding yeast, *Saccharomyces cerevisiae*. J. Cell Biol. *167*, 519–530.

Humphries, C. L., Balcer, H. I., D'Agostino, J. L., Winsor, B., Drubin, D. G., Barnes, G., Andrews, B. J., and Goode, B. L. (2002). Direct regulation of Arp2/3 complex activity and function by the actin binding protein coronin. J. Cell Biol. *159*, 993–1004.

Idrissi, F. Z., Grotsch, H., Fernandez-Golbano, I. M., Presciatto-Baschong, C., Riezman, H., and Geli, M. I. (2008). Distinct acto/myosin-I structures associate with endocytic profiles at the plasma membrane. J. Cell Biol. *180*, 1219–1232.

Jourdain, I., Gachet, Y., and Hyams, J. S. (2009). The dynamin related protein Dnm1 fragments mitochondria in a microtubule-dependent manner during the fission yeast cell cycle. Cell Motil. Cytoskelet. *66*, 509–523.

Jourdain, I., Sontam, D., Johnson, C., Dillies, C., and Hyams, J. S. (2008). Dynamin-dependent biogenesis, cell cycle regulation and mitochondrial association of peroxisomes in fission yeast. Traffic *9*, 353–365.

Kaksonen, M., Sun, Y., and Drubin, D. G. (2003). A pathway for association of receptors, adaptors, and actin during endocytic internalization. Cell *115*, 475–487.

Kaksonen, M., Toret, C. P., and Drubin, D. G. (2005). A modular design for the clathrin- and actin-mediated endocytosis machinery. Cell *123*, 305–320.

Kaksonen, M., Toret, C. P., and Drubin, D. G. (2006). Harnessing actin dynamics for clathrin-mediated endocytosis. Nat. Rev. Mol. Cell Biol. *7*, 404–414.

Kanbe, T., Kobayashi, I., and Tanaka, K. (1989). Dynamics of cytoplasmic organelles in the cell cycle of the fission yeast *Schizosaccharomyces pombe*: three-dimensional reconstruction from serial sections. J. Cell Sci. *94*(Pt 4), 647–656.

Kirchhausen, T. (2009). Imaging endocytic clathrin structures in living cells. Trends Cell Biol. *19*, 596–605.

Lin, M. C., Galletta, B. J., Sept, D., and Cooper, J. A. (2010). Overlapping and distinct functions for cofilin, coronin and Aip1 in actin dynamics in vivo. J. Cell Sci. *123*, 1329–1342.

Merrifield, C. J. (2004). Seeing is believing: imaging actin dynamics at single sites of endocytosis. Trends Cell Biol. *14*, 352–358.

Merrifield, C. J., Perrais, D., and Zenisek, D. (2005). Coupling between clathrin-coated-pit invagination, cortactin recruitment, and membrane scission observed in live cells. Cell *121*, 593–606.

Mulholland, J., Preuss, D., Moon, A., Wong, A., Drubin, D., and Botstein, D. (1994). Ultrastructure of the yeast actin cytoskeleton and its association with the plasma membrane. J. Cell Biol. *125*, 381–391.

Newpher, T. M., Idrissi, F. Z., Geli, M. I., and Lemmon, S. K. (2006). Novel function of clathrin light chain in promoting endocytic vesicle formation. Mol. Biol. Cell *17*, 4343–4352.

Newpher, T. M., and Lemmon, S. K. (2006). Clathrin is important for normal actin dynamics and progression of Sla2p-containing patches during endocytosis in yeast. Traffic *7*, 574–588.

Newpher, T. M., Smith, R. P., Lemmon, V., and Lemmon, S. K. (2005). In vivo dynamics of clathrin and its adaptor-dependent recruitment to the actin-based endocytic machinery in yeast. Dev. Cell *9*, 87–98.

Okreglak, V., and Drubin, D. G. (2010). Loss of Aip1 reveals a role in maintaining the actin monomer pool and an in vivo oligomer assembly pathway. J. Cell Biol. *188*, 769–777.

Okreglak, V., and Drubin, D. G. (2007). Cofilin recruitment and function during actin-mediated endocytosis dictated by actin nucleotide state. J. Cell Biol. *178*, 1251–1264.

Pelham, R. J., Jr., and Chang, F. (2001). Role of actin polymerization and actin cables in actin-patch movement in *Schizosaccharomyces pombe*. Nat. Cell Biol. *3*, 235–244.

Pollard, T. D., Blanchoin, L., and Mullins, R. D. (2000). Molecular mechanisms controlling actin filament dynamics in nonmuscle cells. Annu. Rev. Biophys. Biomol. Struct. *29*, 545–576.

Praefcke, G. J., and McMahon, H. T. (2004). The dynamin superfamily: universal membrane tubulation and fission molecules? Nat. Rev. Mol. Cell Biol. *5*, 133–147.

Reider, A., Barker, S. L., Mishra, S. K., Im, Y. J., Maldonado-Baez, L., Hurley, J. H., Traub, L. M., and Wendland, B. (2009). Syp1 is a conserved endocytic adaptor that contains domains involved in cargo selection and membrane tubulation. EMBO J. *28*, 3103–3116.

Rodal, A. A., Kozubowski, L., Goode, B. L., Drubin, D. G., and Hartwig, J. H. (2005). Actin and septin ultrastructures at the budding yeast cell cortex. Mol. Biol. Cell *16*, 372–384.

Rothlisberger, S., Jourdain, I., Johnson, C., Takegawa, K., and Hyams, J. S. (2009). The dynamin-related protein Vps1 regulates vacuole fission, fusion and tubulation in the fission yeast, *Schizosaccharomyces pombe*. Fungal Genet. Biol. *46*, 927–935.

Sirotkin, V., Beltzner, C. C., Marchand, J. B., and Pollard, T. D. (2005). Interactions of WASp, myosin-I, and verprolin with Arp2/3 complex during actin patch assembly in fission yeast. J. Cell Biol. *170*, 637–648.

Snaith, H. A., Samejima, I., and Sawin, K. E. (2005). Multistep and multimode cortical anchoring of tea1p at cell tips in fission yeast. EMBO J. *24*, 3690–3699.

Stimpson, H. E., Toret, C. P., Cheng, A. T., Pauly, B. S., and Drubin, D. G. (2009). Early-arriving Syp1p and Ede1p function in endocytic site placement and formation in budding yeast. Mol. Biol. Cell *20*, 4640–4651.

Sun, Y., Carroll, S., Kaksonen, M., Toshima, J. Y., and Drubin, D. G. (2007). PtdIns(4,5)P2 turnover is required for multiple stages during clathrin- and actin-dependent endocytic internalization. J. Cell Biol. *177*, 355–367.

Sun, Y., Martin, A. C., and Drubin, D. G. (2006). Endocytic internalization in budding yeast requires coordinated actin nucleation and myosin motor activity. Dev. Cell *11*, 33–46.

Takagi, T., Ishijima, S. A., Ochi, H., and Osumi, M. (2003). Ultrastructure and behavior of actin cytoskeleton during cell wall formation in the fission yeast *Schizosaccharomyces pombe*. J. Electron. Microsc. *52*, 161–174.

Toshima, J., Toshima, J. Y., Duncan, M. C., Cope, M. J., Sun, Y., Martin, A. C., Anderson, S., Yates, J. R., 3rd, Mizuno, K., and Drubin, D. G. (2007). Negative regulation of yeast Eps15-like Arp2/3 complex activator, Pan1p, by the Hip1R-related protein, Sla2p, during endocytosis. Mol. Biol. Cell *18*, 658–668.

Toshima, J. Y., Toshima, J., Kaksonen, M., Martin, A. C., King, D. S., and Drubin, D. G. (2006). Spatial dynamics of receptor-mediated endocytic trafficking in budding yeast revealed by using fluorescent alpha-factor derivatives. Proc. Natl. Acad. Sci. USA *103*, 5793–5798.

Wu, J. Q., McCormick, C. D., and Pollard, T. D. (2008). Chapter *9*, Counting proteins in living cells by quantitative fluorescence microscopy with internal standards. Methods Cell Biol. *89*, 253–273.

Wu, J. Q., and Pollard, T. D. (2005). Counting cytokinesis proteins globally and locally in fission yeast. Science *310*, 310–314.

Wu, J. Q., Sirotkin, V., Kovar, D. R., Lord, M., Beltzner, C. C., Kuhn, J. R., and Pollard, T. D. (2006). Assembly of the cytokinetic contractile ring from a broad band of nodes in fission yeast. J. Cell Biol. *174*, 391–402.

Young, M. E., Cooper, J. A., and Bridgman, P. C. (2004). Yeast actin patches are networks of branched actin filaments. J. Cell Biol. *166*, 629–635.

Zacharias, D. A., Violin, J. D., Newton, A. C., and Tsien, R. Y. (2002). Partitioning o lipid-modified monomeric GFPs into membrane microdomains of live cells. Science *296*, 913–916.